DEGREE PROJECT IN ENGINEERING PHYSICS,
SECOND CYCLE, 30 CREDITS
STOCKHOLM, *SWEDEN 2020*

A scaling approach to critical exponent calculations for the 2D Ising model

THOM JÄDERLUND

KTH ROYAL INSTITUTE OF TECHNOLOGY
SCHOOL OF ENGINEERING SCIENCES

Master of Science Thesis

A scaling approach to critical exponent calculations for the 2D Ising model

Thom Jäderlund

Condensed Matter, Department of Theoretical Physics,
School of Engineering Sciences
Royal Institute of Technology, SE-106 91 Stockholm, Sweden

Stockholm, Sweden 2020

Typeset in LaTeX

Akademisk avhandling för avläggande av teknologie masterexamen inom ämnesområdet teoretisk fysik.

Scientific thesis for the degree of Master of Science in Engineering in the subject area of Theoretical physics.

TRITA-SCI-GRU 2020:043

Printed in Sweden by Universitetsservice US AB, Stockholm May 2020

Abstract

We use a scaling argument combined with Kadanoff block spins for the Monte Carlo renormalisation group to determine the critical exponent y_h. The critical exponent is calculated from both the magnetisation and magnetic susceptibility, at T_c, which are acquired from Monte Carlo simulations of a 2D Ising model. We investigate different summation rules for the block spins and compare the critical exponent for these to that of finite size scaling. A critical exponent estimate was considered satisfactory if it rounded to four correct significant figures. For the magnetisation, renormalisation yielded no benefit compared to the finite size scaling, whereas for susceptibility improvement was noticed. The various block spin rules also performed differently well, based on which thermodynamic quantity that was investigated.

Key words: Critical exponent, Ising model, Renormalisation group, Scaling, Monte Carlo simulations, Wolff algorithm.

Sammanfattning

Vi använder ett skalningsargument kombinerat med Kadanoff blockspinn för Monte Carlo renormaliseringsgruppen för att bestämma den kritiska exponenten y_h. Den kritiska exponenten bestäms från både magnetiseringen och magnetiska susceptibiliteten, vid T_c, vilka erhålls från en Monte Carlo simulering av en 2D Isingmodell. Vi undersöker olika summeringsregler för blockspinnen och jämför den kritiska exponenten för dessa med den från s.k. finite size scaling. En kritisk exponentuppskattning klassades som god om den avrundades till fyra korrekta värdesiffror. För magnetiseringen gav renormaliseringen ingen förbättring jämfört med finite size scaling, men för susceptibiliteten ledde renormaliseringen till fler goda resultat. De olika blockspinnreglerna fungerade olika bra, baserat på vilken termodynamisk storhet som undersöktes.

Nyckelord: Kritiska exponenter, Isingmodellen, Renormaliseringsgruppen, Skalning, Monte Carlo simuleringar, Wolffalgoritmen.

Preface

This thesis is based on work carried out from June 2019 to April 2020 at the Department of Physics at the Royal Institute of Technology, KTH. The project was supervised by Associate Professor Jack Lidmar.

Overview

The thesis is composed of six chapters, structured as follows: chapter one touches on the history of the Ising model and its connections to phase transitions and the renormalisation group. In the second chapter, the Ising model is studied in more detail through its mathematical definition and we investigate some of the observables to the model. The third chapter focuses on the Monte Carlo renormalisation group, by investigating block spins, critical exponents and finally deriving the scaling approach used in this thesis. Chapter four describes the numerical model as well as the different block spin rules used when running the simulations. In chapter five, the results are presented separately for the magnetisation and susceptibility. Chapter six concludes the thesis with a summary and conclusion.

Acknowledgements

First and foremost, I would like to thank Associate Professor Jack Lidmar for his patience and guidance throughout this project. I am grateful having been allowed to explore the interesting fields of renormalisation and simulation independently, yet helping me with long discussions surrounding the topic whenever needed.

I would also like to express my most humble gratitude to my parents Annika and Peter, and my sister Lisa. You have been with me throughout this entire journey, believing and supporting me, especially in times when I

did not. Without you, this thesis would not have finished, and I would not be where I am today. Thank you for always being there.

Stockholm, April 2020

Contents

Chapter 1

Introduction

One hundred years ago, Wilhelm Lenz published a model for magnetic properties in solid bodies [1]. It was later given to Ernst Ising, from whom the name derives, who in his doctoral thesis solved the one-dimensional case [2]. It was not until 1944 that Lars Onsager [3] managed to prove an analytical solution for the two-dimensional case, which has phase transitions. The existence of phase transitions for dimensions larger or equal to 2 was shown by Rudolf Peierls in 1936 [4]. While analytical solutions exist for the one- and two-dimensional cases, no such solutions have been found for the three-dimensional or higher. In the latter, one has to rely on methods such as numerical simulations.

While a relatively simple model, the Ising model, as aforementioned, exhibits phase transitions in higher dimension than one. Accompanied by the rapid advancement of computers during the later half of the nineteenth century, modelling of these system became ever more common. And with faster computers came the possibility to simulate larger systems, from which the phase transitions can be studied.

Phase transitions are perhaps the first physical reaction we come in contact with in the world. Seeing water evaporate into gas, or freeze into ice are observations of these everyday transitions. These are examples of $first$ - $order$ phase transitions, so called due to them having a discontinuity in the first derivative of the corresponding thermodynamic quantity [5]. In water, the change in volume from its liquid to gaseous state, or solid to liquid state, requires an excess latent heat be transferred [6].

On the other hand, there are *second* - *order* phase transitions, also called *continuous* phase transitions, that occur without the discontinuity in

the first derivative of the thermodynamic quantity, and the phases may continuously transition between the separate phases. These are called *critical points*, points where only incremental changes to a quantity can completely change the phase of a substance. For water, a critical point exists where the difference between gaseous and liquid state disappears. This point is at $T_c = 647.096$ K and $P_c = 22.064$ MPa [7].

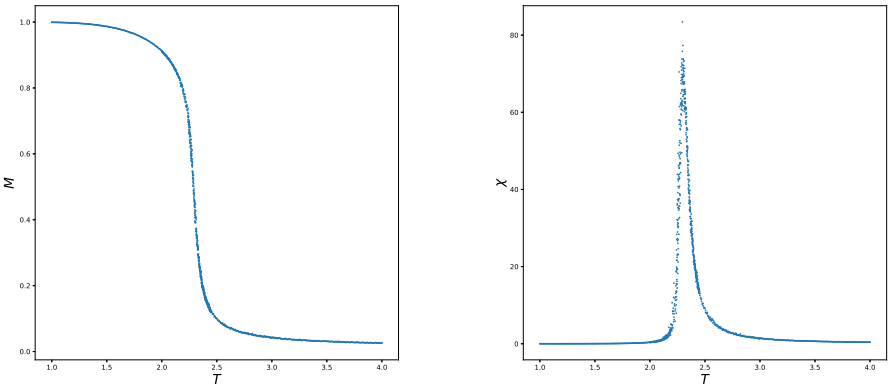

(a) Magnetisation against temperature. (b) Susceptibility against temperature.

Figure 1.1: Absolute magnetisation and magnetic susceptibility for a 64×64 2D Ising system. Extra simulations carried out between $T = 2.4$ and $T = 2.5$. Plots indicate a continuous transition from a magnetic to non-magnetic state, while the susceptibility shows a divergence.

Through the use of toy models, such as the Ising model, and numerical simulations, one may determine the critical temperature for the various thermodynamic quantities, despite their simplicity. Finding these points, in turn, makes it possible to determine the *critical exponents*; exponents governing phase transitions.

While understanding of the physics around theses points is interesting in and of itself, the critical exponents carries a potential broader significance. In the description of critical points by Griffiths [8] it is shown that they are dependent on the dimensionality of the system, the symmetry of the model, *i.e.* square lattice, spherical model, etc. and also the range of the interactions. In order to understand behaviours, one may use the the *renormalisation group*, RG, [9].

The idea behind renormalisation is finding some method to forgo the short-range behaviour of a system. In this thesis, the system is the Ising model, and the method is a so called *block spin* transformation developed by Kadanoff [10]. By one renormalisation iteration, all spins in the block are effectively reduced to one single value, reducing the degrees of freedom from the size of the block to one.

Through successive iterations, the Hamiltonian of the system is distilled from its short-range behaviour and left only with the long-range one, ultimately terminating in a fixed point. This is called the *renormalisation group flow*, and as the Hamiltonian remains invariant under the transformation [11], we end up with an effective Hamiltonian, where the long-range behaviour remains unchanged.

The implications of this are grand. If the RG flow flows into a fixed point, which it does if at the critical temperature, T_c, the Hamiltonian will share the critical exponents with the model it came from *e.g.* the Ising model. The concept that several Hamiltonians, flowing into the same critical point share critical exponents is called *universality*.

This thesis will focus on the 2D Ising model and its critical exponents. While we already through analytical means know the exact values for this model, this knowledge may be used to investigate the validity of other aspects such as renormalisation. Here we will examine the effect of different block spin rules on the calculation of critical exponents and comparing them to finite size scaling.

Finding different block spin rules is of interest, as one of the most common rules converges very slowly for the 3D Ising model [12], where we have to rely on numerical methods to determine the critical exponents. We combine our different block spin rules with another approach in calculating the critical exponents, namely through scaling of the thermodynamic quantities [13], [14].

Chapter 2

The Ising Model

2.1 Mathematical Background

The Ising model is built around the spin σ_i of site i and its interaction with a neighbouring spin σ_j of site j with an interaction term J_{ij} connecting the two [11]. These are combined into the Hamiltonian for the Ising model as

$$\hat{H}(\sigma) = -\sum_{\langle i,j \rangle} J_{ij}\sigma_i\sigma_j, \tag{2.1}$$

where $\langle i, j \rangle$ implies summation over nearest neighbour sites. This may further be built upon the inclusion of an external magnetic field H

$$\hat{H}(\sigma) = -\sum_{\langle i,j \rangle} J_{ij}\sigma_i\sigma_j - \sum_i H_i\sigma_i \tag{2.2}$$

One does not necessarily need to stop at nearest neighbour interaction, but can also sum over next nearest neighbour, four spin and so forth. Let us consider these different interactions as $\psi_\alpha(\sigma_i)$ and for the sake of simplicity assume $h = 0$ and we now have

$$\hat{H}(\sigma) = -\sum_\alpha J_\alpha \psi_\alpha(\sigma_i). \tag{2.3}$$

This can be further simplified by multiplying (1.3) by $-\beta$ and redefining $-\beta J_\alpha = K_\alpha$ as

$$\tilde{H}(\sigma) = -\beta\hat{H}(\sigma) = \sum_\alpha K_\alpha \psi_\alpha(\sigma_i). \tag{2.4}$$

2.2 Observables

2.2.1 Partition function

Let us recall the definition of the partition function Z [6]

$$Z = \sum_n e^{-\beta E_n}, \tag{2.5}$$

where β is the inverse thermodynamic temperature, $\beta = (k_b T)^{-1}$ and E_α the total energy of the system and consider the energy eigenstates [15]

$$\hat{H} |n\rangle = E_n |n\rangle \tag{2.6}$$

yielding

$$Z = \sum_n e^{-\beta E_n} = \mathrm{Tr}\left(e^{-\beta \hat{H}}\right). \tag{2.7}$$

Combining this result with 1.4 we get

$$Z = \mathrm{Tr}\left(e^{\tilde{H}}\right). \tag{2.8}$$

2.2.2 Magnetisation and Magnetic Susceptibility

One of the easiest properties to determine, especially numerically, is the magnetisation per spin, M. This is simply given by

$$M = \frac{1}{N} \sum_i^N \sigma_i, \tag{2.9}$$

with N being the amount of sites. For a square lattice one simply replaces N by L^2, where L is the lattice length.

Another function we chose to investigate was the variance of the magnetisation

$$\mathrm{Var}(M) = \left\langle M^2 \right\rangle - \langle M \rangle^2, \tag{2.10}$$

since this can be easily computed at the same time. Further, it may be realised that this is in fact proportional to the magnetic susceptibility, χ of the system [6]

$$\chi = \beta \left(\left\langle M^2 \right\rangle - \langle M \rangle^2 \right) \tag{2.11}$$

2.2.3 Connection to free energy

We may also express the magnetisation using the change in free energy for a magnetic system as [6]

$$\mathrm{d}F = -S\mathrm{d}T - M\mathrm{d}H, \tag{2.12}$$

which in the isothermal case yields

$$M = -\left(\frac{\partial F}{\partial H}\right)_T, \tag{2.13}$$

and since the magnetic susceptibility, χ, is defined as

$$\chi = \left(\frac{\partial M}{\partial H}\right)_T, \tag{2.14}$$

we also have

$$\chi = -\left(\frac{\partial^2 F}{\partial H^2}\right)_T. \tag{2.15}$$

Chapter 3

Monte Carlo renormalisation group

3.1 Kadanoff block spin

In 1966, Kadanoff proposed a lattice renormalisation based on blocks [10]. Assuming a lattice with length L and of dimension d, it is divided into blocks of size b^d, where b is the length of the block. Each block contains a set of spins, which are to be evaluated according to a block rule.

Once a block has been evaluated, the block is transformed to a single lattice point with the value the block rule led to. When all blocks are evaluated, a new renormalised lattice is created from them, changing the dimension by a factor b^{-d}. This is most easily described visually in figure 3.1.

3.2 Critical exponents

Near the critical temperature T_c, several physical properties obey a power law dependence on $|T - T_c|$. Critical exponents are commonly labelled $\alpha, \beta, \gamma...$ for $T < T_c$, each corresponding to a specific physical quantity [5]. For $T > T_c$, the exponents are commonly accompanied by a prime. The exponents describe phase transitions of these quantities usually near a critical temperature T_c.

For a magnetic system, the second exponent, β, is the easiest to conceptualise. β, corresponding to the order parameter of the system, which in a magnetic system is the magnetisation [11]. Thus, what β describes

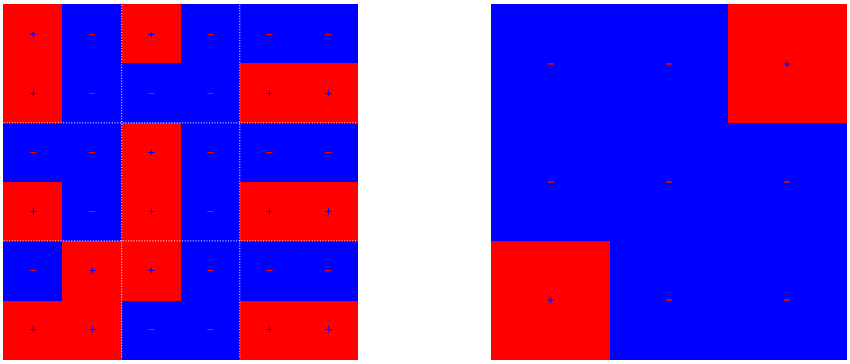

(a) Lattice prior to renormalisation. (b) Lattice after renormalisation.

Figure 3.1: Renormalisation of the left lattice, (a), where $L = 6$, utilising the majority rule 3.2.1 for Kadanoff block spins with $b = 2$. The white dashed lines indicate the block spin divisions. The Renormalised lattice, (b), on the right with $L = 3$.

is the behaviour when the system spontaneously magnetises. Assuming no external magnetic field

$$M(T, H = 0) = M_0(T) \sim (T_c - T)^{\beta}, \quad T < T_c. \tag{3.1}$$

The value for β was found to be $\beta = 1/8$ for the 2D Ising model [16]. Similarly, we have the susceptibility as

$$\chi(T, H = 0) = \chi_0(T) \sim |T - T_c|^{-\gamma}, \quad T < T_c. \tag{3.2}$$

In general, it is assumed that critical phenomena for thermodynamic quantities are governed by similar power laws [15] associated with the reduced temperature

$$X \sim t^x = \left(\frac{T - T_c}{T_c} \right)^x, \tag{3.3}$$

for $T < T_c$, where x is the critical exponent to the arbitrary thermodynamic quantity X.

3.2.1 2D Ising critical exponents

Here we list the the critical exponents when $H = 0$ for the 2D Ising model. The 2D Ising values [10] are exact. 3D Ising values included for comparison [17] and are numerical estimates :

Physical Quantity	Critical Exponent	2D Ising	3D Ising
Specific heat	α	0	0.1096
Magnetisation	β	1/8	0.32653
Susceptibility	γ	7/4	1.2373
	δ	15	4.7893
Correlation length	ν	1	0.63012
	η	1/4	0.03639

Table 3.1: Values of various critical exponents for a 2D and 3D Ising model, in the absence of an external magnetic field, $H = 0$. The 2D values are exact, while the 3D are approximate.

3.2.2 Scaling laws

Combinations of the various relations yields several so called *scaling laws*. Amongst the most known is the Rushbrooke inequality [18]. We consider the response function

$$C_H - C_M = \frac{T}{\chi_H}\left(\frac{\partial M}{\partial T}\right)_H^2 . \tag{3.4}$$

As the heat capacity is a positive value, we may create the inequality

$$C_H \geq \frac{T}{\chi_H}\left(\frac{\partial M}{\partial T}\right)_H^2 . \tag{3.5}$$

We now have three quantities we know the exponents for

$$\begin{aligned} C_H &\sim |T - T_c|^{-\alpha}, \\ \chi_H &\sim |T - T_c|^{-\gamma}, \\ M &\sim (T_c - T)^{\beta}, \\ \frac{\partial M}{\partial T} &\sim (T_c - T)^{\beta - 1}. \end{aligned} \tag{3.6}$$

With $T < T_c$ in our case, we may express (3.5) as

$$\begin{aligned} (T_c - T)^{-\alpha} &\geq T(T_c - T)^{\gamma}(T_c - T)^{2(\beta-1)}, \\ (T_c - T)^{-\alpha-2\beta-\gamma+2} &\geq T. \end{aligned} \tag{3.7}$$

Investigating the limit as $T \to T_c$, we find that the exponential terms cannot be larger than zero

$$\begin{aligned} -\alpha - 2\beta - \gamma + 2 &\leq 0, \\ \alpha + 2\beta + \gamma &\geq 2. \end{aligned} \tag{3.8}$$

This is the so called Rushbrooke inequality.

Several other inequalities have been derived. Some of the more common are listed below.

Widom inequality [19]

$$\gamma \geq \beta(\delta - 1). \tag{3.9}$$

Griffiths inequality [20]

$$(1 + \delta)\beta \geq 2 - \alpha. \tag{3.10}$$

Fisher inequality [21]

$$\gamma \leq (2 - \eta)\nu. \tag{3.11}$$

3.2.3 Universality

One fascinating thing that comes to mind when investigating the aforementioned scaling inequalities is, when plugging in the exact solutions from the 2D Ising model, we find that the inequalities holds as equalities. The same seems to be true for the 3D case, why it is not difficult to assume that equality always holds, though it has not been proven.

3.3 A scaling approach to renormalisation

In order to calculate the critical exponents, the RG flow must be approximated in some way. The approximation may be conducted by either analytical methods or numerical simulations, the most common method is the latter combined with finite size scaling.

When it comes to Monte Carlo renormalisation group, MCRG, the method established by Swendsen has traditionally been used, [22], [23], [24], [25] amongst others. Another approach was put forth by Kikuchi and Okabe, [13], focusing on changes in the thermodynamic quantities. Considering the free energy during one renormalisation iteration [14]

$$F(t,h) = b^{-d}F(b^{y_t}t, b^{y_h}h), \tag{3.12}$$

with b according to Kadanoff, d is the dimension, and with

$$t = \frac{T - T_c}{T_c}, \qquad h = \beta H. \tag{3.13}$$

Using equation (1.13) and (1.15), we can now define a scaling approach to the renormalisation iterations

$$M = b^{y_h - d}M(b^{y_t}t, b^{y_h}h), \tag{3.14}$$

and

$$\chi = b^{2y_h - d}\chi(b^{y_t}t, b^{y_h}h). \tag{3.15}$$

Consider renormalisation iterations n, m where $n < m$, combined with their respective fields χ_n and χ_m. By combining these two, we may derive an expression for the critical exponent y_h from the susceptibility

$$\frac{\chi_n}{\chi_m} = b^{(n-m)(d-2y_h)}, \tag{3.16}$$

yielding

$$y_h = \frac{1}{2}\left(d - \frac{\ln(\chi_n) - \ln(\chi_m)}{\ln(b^n) - \ln(b^m)}\right), \tag{3.17}$$

or the case for the magnetisation

$$y_h = d - \frac{\ln(M_n) - \ln(M_m)}{\ln(b^n) - \ln(b^m)}. \tag{3.18}$$

Comparing to the magnetic susceptibility for the 2D Ising model, which scaled according to $\sim |T - T_c|^{-\gamma}$, we may determine a numerical value for y_h, from the original critical exponents

$$\begin{aligned} d - 2y_h &= -\gamma/\nu, \\ y_h &= 1.875. \end{aligned} \tag{3.19}$$

Chapter 4

Numerical model

Each initial lattice generated was one in a disordered state, with no or very small absolute magnetisation. The size of the non-renormalised lattice was 512×512 sites, and we made use of periodic boundary conditions. The critical temperature value used was $T_c = 2.26918531421$.

Coding for this thesis was made in Python 3 utilising the Anaconda distribution and built-in NumPy package.

4.1 Lattice update algorithm

Single-spin Monte Carlo simulations, e.g. the Metropolis-Hastings algorithm [26], suffered from one major drawback when investigating phase transitions. When nearing the critical temperature, T_c, of a system, the simulation would suffer from a critical slowing down [27] and for a square lattice with length L, it grows proportional to L^2.

To circumvent the problem of critical slowing down, Swendsen and Wang presented a method of flipping a cluster of spins, rather than a single spin [27]. This yielded a faster algorithm for systems larger than 18×18. Building on their work, Wolff made further improvements [28], yielding the algorithm used in this thesis.

4.1.1 Wolff algorithm

The Wolff algorithm can be described by four steps:

(i) Randomly select a lattice site, i, determine the spin of i, S_i, and add i to the cluster.

(ii) Investigate all nearest neighbour sites j to i. If $S_j = S_i$, add j to the cluster with a probability of $p = 1 - \exp(-2J\beta)$. When all nearest neighbours have been investigated, flip the spin of i, $S_i \to -S_i$, and remove i from the cluster.

(iii) Repeat step (ii) for the new sites added to the cluster.

(iv) When no new sites may be added to the cluster and the cluster is empty, repeat step (i).

4.1.2 Parameters

As the purpose of this thesis is to investigate forms of renormalising the lattice, we chose to use $J = 1$ and $k_b = 1$, which yielded the spin flip probability $p = 1 - \exp(-2/T)$. An important part when running Monte

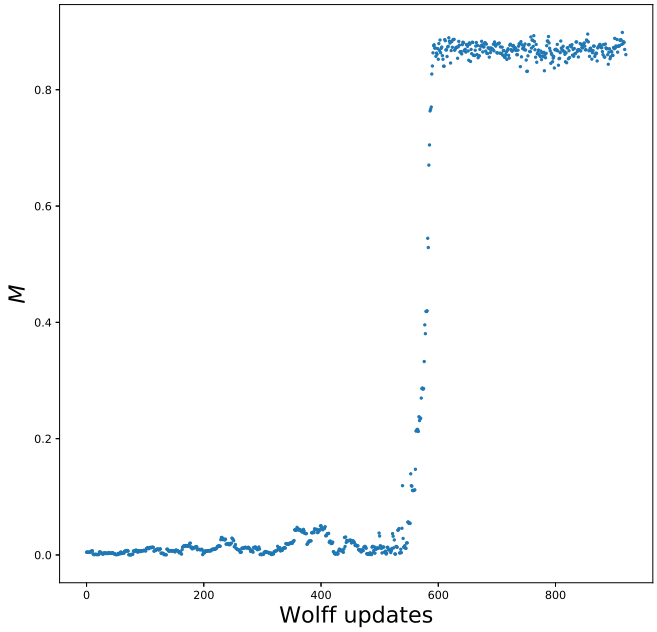

Figure 4.1: Magnetisation against Wolff updates. $L = 128$ and $T = 2.1$.

Carlo simulations is choosing when to stop equilibration of the initial system and start taking measurements [29].

Determining equilibration a posteriori, as can be seen from figure 4.1, occurred around 550 updates. The amount of steps required varies for each run and also due to lattice size, L^2 and temperature, T. Thus, we are required to find a function independent of lattice size, temperature and individual run equilibration time.

Although M equilibrates around a given value, the fluctuations are relatively large, as can be seen in Figure 4.1. Finding a less fluctuating value will be more favourable. Upon investigating figure 4.2, we realise that the

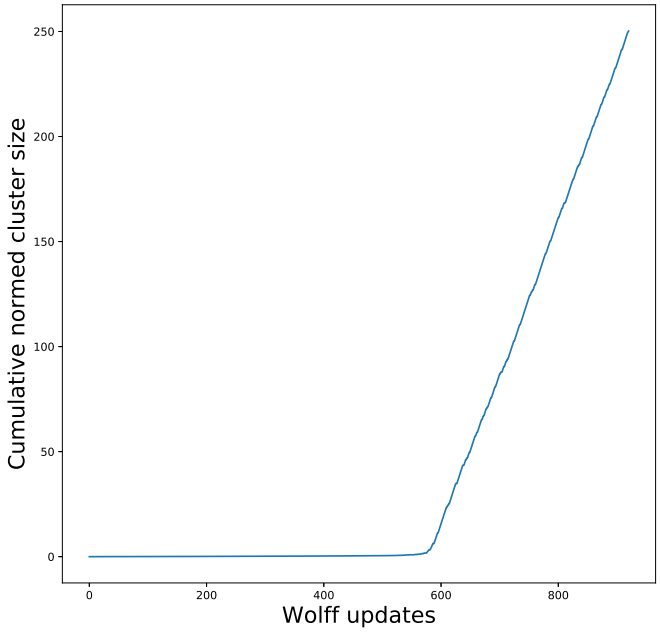

Figure 4.2: Cumulative normed cluster size against Wolff updates. The cluster size is normed by the system size, to avoid large numbers. $L = 128$ and $T = 2.1$.

change in cumulative normed cluster size becomes linear after equilibration, corresponding to a constant cluster size.

To determine if equilibrium had been reached, we define

$$\Delta c = \frac{c_{s+n}}{c_s}, \tag{4.1}$$

where c_s is the cluster size at s steps and c_{s+n} the cluster size n steps later. Equilibrium is assumed to have been achieved when

$$0.999 < \Delta c < 1.000. \tag{4.2}$$

The motivation for $\Delta c < 1.000$ was to avoid accepting values for the initial small clusters seen before 550 steps in figure 4.2. One could impose a limit on cluster size, but that would pose a problem at higher temperatures, when the cluster sizes were much smaller.

For the simulations, we computed Δc every tenth step, and used $n = 10$. The process time for reaching equilibrium was measured, and subsequent measurements were taken for the same time - ensuring an equal divide between equilibrium and measurements CPU time [29].

The measurements were taken at T_c, since it is at this temperature the simulations take the longest to equilibrate. Averaging over the results, it is used to determine the amount of spin flips per spin, SFPS, during the renormalisation simulations. The results from 1000 simulations yielded 195 SFPS on average for equilibration. From this, we concluded to run the simulations presented in table 4.1.

Simulation	Equilibrium	Measurement	Total
$T_c - 0.02$	250	250	500
$T_c - 0.01$	250	250	500
T_c	250	250	500
$T_c + 0.01$	250	250	500
$T_c + 0.02$	250	250	500

Table 4.1: Amount of spin flips per spin, SFPS, used during the simulations. An extra 55 was added as a margin.

In the paper by Ron, Brandt and Swendsen, [12], they used 420 SFPS for a 64^3 system. As $64^3 = 512^2$, using 500 SFPS felt reasonable. As one SFPS constitutes of $L^2 = 512^2$ spin flips, and each call in the Wolff algorithm flips a cluster of spins, we also measure how many additional spin flips that was conducted on average.

SFPS	M	σ_M	χ	σ_χ
500	0.19755	0.00684	487.66	29.179
1000	0.19937	0.00538	491.66	18.457

Table 4.2: Results for proof of concept run. The magnetisation, M, and susceptibility, χ, are the averages of 100 runs. σ denotes the standard deviation.

As a proof of concept, we investigated the impact of a doubling of the amount of equilibrium and measurement SFPS. The simulations were run at $T = T_c$+0.02 and 100 data points were gathered for the two runs respectively. The results are presented in table 4.2. It shows that the extra runs did not significantly improve the results, as the quantities M and χ lies well within the respective standard deviation, σ.

4.2 Renormalisation method and rules

The renormalisation of the lattice is conducted by dividing it into square block spins. The blocks are subjected to block spin transformations according to the rules presented below. The size of the blocks were 2×2, i.e. the scale factor was $b = 2$.

4.2.1 Majority rule

The majority rule, MJ , has been thoroughly investigated, amongst other by Swendsen in 1979 [22] and has been shown to perform well. Here it was used as a baseline. The block spin, S, is calculated from the sum of spins inside the block. It is most easily demonstrated graphically.

Consider the 2×2 block in figure 4.3. The majority rule works by taking the sum of all spins inside the block, and investigating the sign of the sum. In the case of figure 4.3, the sum is -2, why the majority rule transforms the block into a negative spin. We may also notice how the degrees of freedom are reduced from four to one.

One problem occurred if the sum is equal to zero. In that case, the spin was randomised with a 50% probability of either $S = 1$ or $S = -1$ [24].

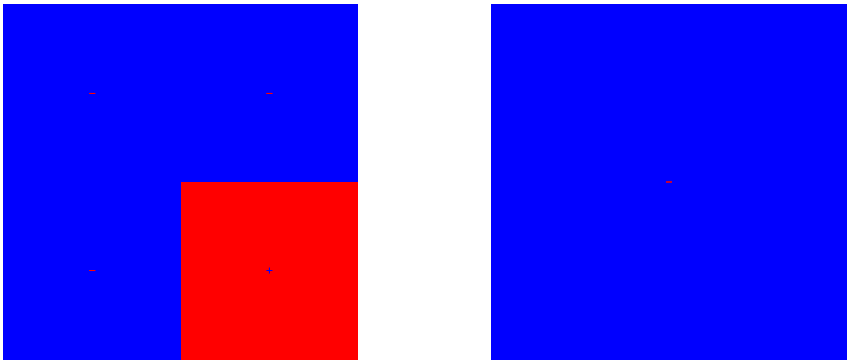

(a) Initial block. (b) Renormalised block.

Figure 4.3: Renormalisation of a 2×2 block according to the majority rule.

4.2.2 Modified Majority rule

The modified majority rule, MZ, works on the same basis as the regular majority rule, albeit with one difference. If we renormalised more than once, we allow $S = 0$ instead of randomising it, until the last renormalisation iteration.

4.2.3 Probabilistic nearest neighbour rule

The probabilistic nearest neighbour rule, NN, is constructed similarly to the majority rule, but instead of being deterministic it was probabilistic. For each block, we construct the two probabilities from the spins S_i as

$$\begin{aligned} p_+ &= b^{-2} \sum_{\langle + \rangle} S_i, \\ p_- &= b^{-2} \sum_{\langle - \rangle} S_i, \end{aligned} \tag{4.3}$$

where $\langle + \rangle$ implies the sum is to be carried over all positive spins within a block, and conversely $\langle - \rangle$ to be the sum of all negative spins. The block spin is set as $S = 1$ with a probability p_+, or $S = -1$ with a probability of p_-.

Should the spin distribution be equal, we note that the rule was the same as for the majority rule.

4.2.4 Probabilistic 33 nearest neighbour rule

The probabilistic 33 nearest neighbour rule, $P33$, is constructed similarly as the NN but the block summation part accounts for only 33.33% of the total probability. Here we have

$$\begin{aligned} p_+ &= \frac{1}{3}\left(1 + b^{-2}\sum_{\langle + \rangle} S_i\right), \\ p_- &= \frac{1}{3}\left(1 + b^{-2}\sum_{\langle - \rangle} S_i\right), \end{aligned} \tag{4.4}$$

4.2.5 Probabilistic 50 nearest neighbour rule

The probabilistic 50 nearest neighbour rule, $P50$, is constructed similarly as the $P33$ but the block summation part accounts for only 50% of the total probability. Here we have

$$\begin{aligned} p_+ &= \frac{1}{2}\left(\frac{1}{2} + b^{-2}\sum_{\langle + \rangle} S_i\right), \\ p_- &= \frac{1}{2}\left(\frac{1}{2} + b^{-2}\sum_{\langle - \rangle} S_i\right), \end{aligned} \tag{4.5}$$

4.3 Finite size scaling

As a comparison to the renormalisation rules, we also run simulations without conducting renormalisation, and instead generate initial lattices of sizes corresponding to that of the renormalised ones. These are presented as finite size scaling, FZ.

4.4 Critical exponent calculation

For each temperature and renormalisation method, 1000 simulations are run in accordance with table 4.1. In order to determine the statistical accuracy, a

bootstrap method is used to assess the numerical results. A total of 10^4, with one bootstrap being the average of 1000 randomly selected results from our initial simulations. From these we calculate the critical exponents according to equations (3.17) and (3.18) and through these determine the bootstrap variance. The percentage error, PE, is also calculated for the respective bootstrap estimate, defined as

$$PE = \frac{y_h^{exact} - y_h^b}{y_h^{exact}} \cdot 100, \tag{4.6}$$

where y_h^b is the bootstrap estimate of the critical exponent, and y_h^{exact} according to the exact value for the 2D Ising model, (3.19).

A total of 7 renormalisation iterations are conducted for each temperature and renormalisation method, thus the smallest system has the size 4×4.

Chapter 5

Results

Here results from the simulations are presented. They were split into two sections, one for the magnetisation and one for the susceptibility. Full numerical results are presented in appendix A.

Results that laid within $1.8745 \leq y_h < 1.8755$ are specifically presented, as these would have yielded the exact value y_h^{exact} according to (3.19), when rounded to four significant figures. The occurrence of y_h within this limit based on (n, m) was also shown, to see if any combination of iterations stood out.

The RG flow diagrams plotted were for $(n, m) = (n, n+1)$. All exponents (n, m) for all $m > n$, were defined as generation n.

5.1 Magnetisation

5.1.1 Main results

In general, $(n, m) = (5, 7)$ and $(6, 7)$ yielded unfavourable results where the percentage error ranged from $0.2 \rightarrow 0.5$. This could be seen as the slightly upward tilt in the RG flow diagrams. Percentage errors larger than 0.1 usually occurred once or twice per generation of n, either at $(n, n+1)$ or $(n, 7)$. For the stochastic rules, NN, $P33$ and $P50$, all first generation $(n, m) = (1, m)$ resulted in $PE < 0.1$, $m = 7$ included.

The simulations yielded 29 results within the four significant figures interval and are presented in figure 5.1. Five of the 29 belonged to the finite size results, while 24 to the renormalisation methods. Thus, on average the renormalisation methods yielded 4.8 results within four significant number,

while the finite size method provided 5. Four out of five of the finite size results laid in the first generation, *i.e.* $(n, m) = (1, m)$.

The iteration that yielded the closest results was $(n, m) = (1, 5)$. Of particular interest was $P33$, with 10 values within the significant figures interval. Of these $(n, m) = (n, 6)$, for $n = 1, 2, 3, 4, 5$ all laid on the interval. The closest value was $FZ_{13} = 1.874977$.

Of the 29 values, only 5 were smaller than $y_h = 1.875$, which indicated a bias towards larger values. Due to the biased results, no average was calculated.

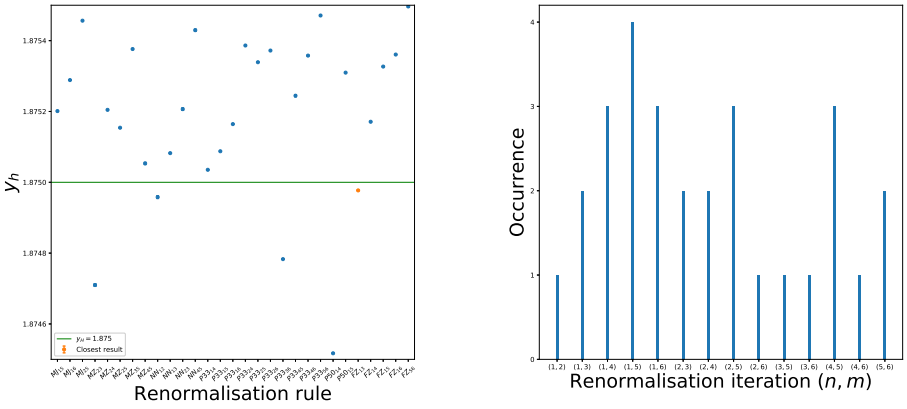

(a) Correct four significant figures.

(b) Occurrence of iterations.

Figure 5.1: Critical exponent $y_h = 1.875$ versus renormalisation rule RR_{nm}, where nm are the renormalisation iteration as described in section 3.3. The error bars (variance) are present, but in general smaller than the circles. In (b) the occurrence of y_h within the specified limit based on renormalisation iterations (n, m), but ignoring renormalisation rule.

5.1.2 RG flow diagrams

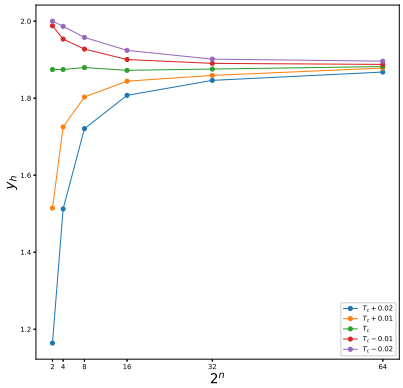

(a) RG flow MJ.

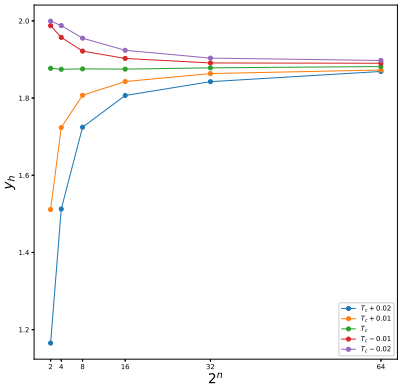

(b) RG flow MZ.

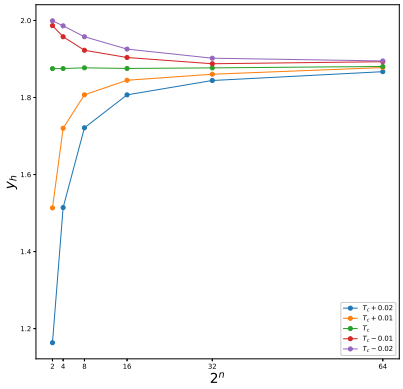

(c) RG flow NN.

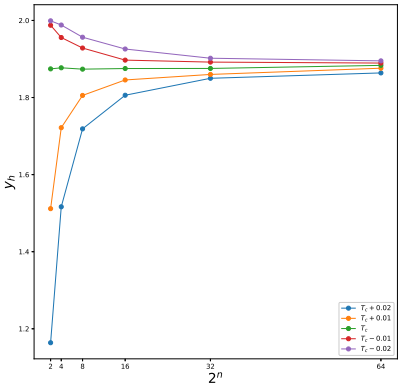

(d) RG flow P33.

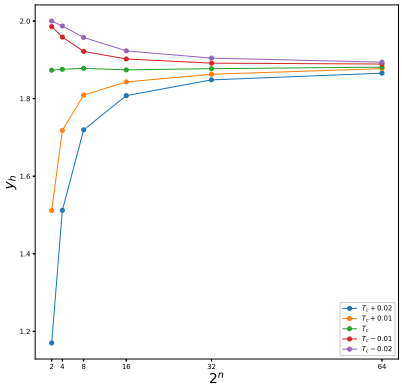

(e) RG flow P50.

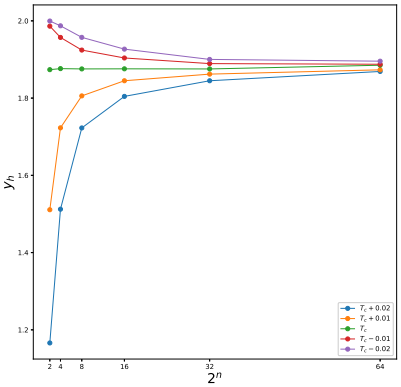

(f) RG flow FZ.

Figure 5.2: RG flow diagrams of the magnetisation for the various block spin rules for $(n, m) = (n, n + 1)$.

5.2 Susceptibility

5.2.1 Main results

Combinations of renormalisation iteration 6 and 7 yielded critical exponents that deviated strongly, and generation 4, 5 and 6 yielded percentage errors larger than 0.1%. This was present for all rules and the finite size case, with the only exception being $P33_{45}$. n or m equal to four also generally led to an off result.

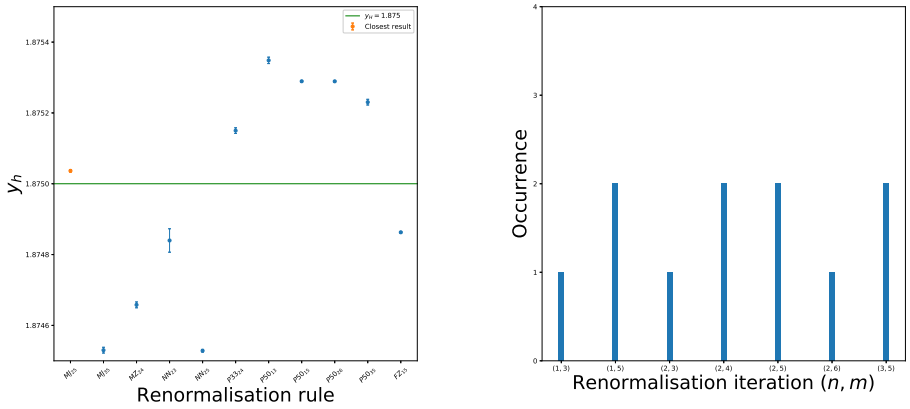

(a) Correct four significant figures.

(b) Occurrence of iterations.

Figure 5.3: Critical exponent $y_h = 1.875$ versus renormalisation rule RR_{nm}, where nm were the renormalisation iteration as described in section 3.3. The error bars indicate the variance. In (b) the occurrence of y_h within the specified limit based renormalisation iterations (n, m), but ignoring renormalisation rule.

The simulations yielded 11 results within the span and are presented in figure 5.5. One of these were the finite size and 10 belonged to the renormalisation methods. On average, the renormalisation methods yielded 2.0 correct y_h, compared to the finite size amount of 1. The finite size results were all in the first generation.

The combinations that yielded the closest results were achieved by $(n, m) = (1, 3)$, $(2, 4)$, $(2, 4)$ and $(3, 5)$ with two entries each. The probabilistic 50 nearest neighbour rule, $P50$ yielded the most entries, while the standard majority rule, MJ_{25}, yielded the single closest value of $y_h = 1.875037$.

Of the 11 results, 6 were below $y_h = 1.875$, and 5 were above, which indicated a higher accuracy. The average of these 11 values were $y_{h,ave} = 1.874978$, thus five significant figures. The percentage error was $PE = 0.001148$, roughly half the one achieved by MZ_{23}.

5.2.2 RG flow diagrams

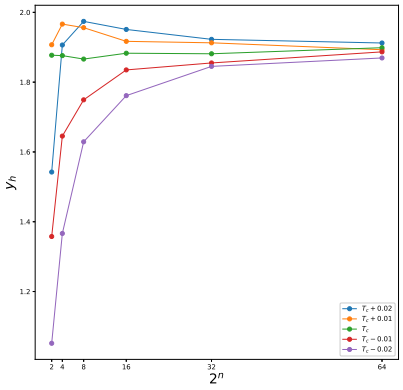

(a) RG flow MJ.

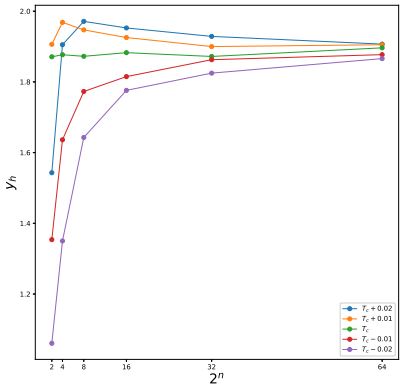

(b) RG flow MZ.

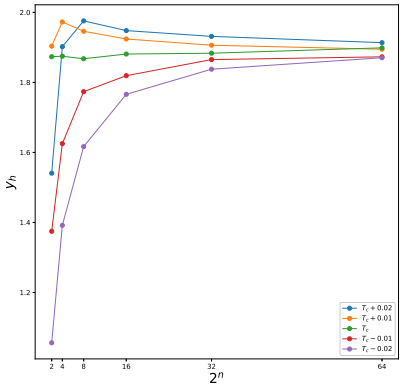

(c) RG flow NN.

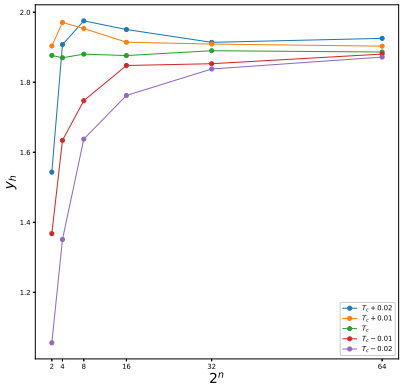

(d) RG flow P33.

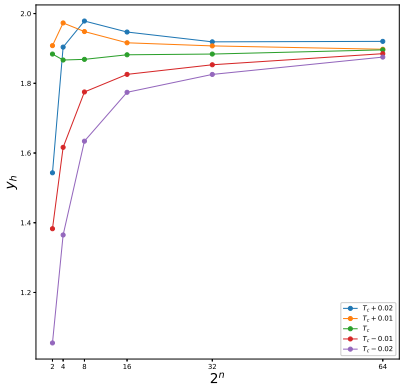

(e) RG flow P50.

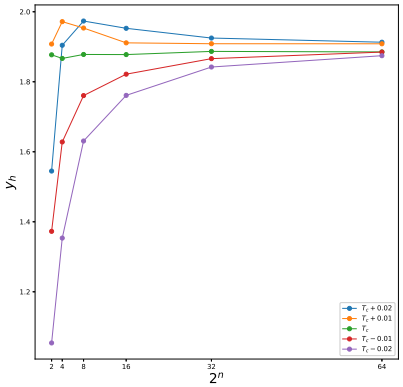

(f) RG flow FZ.

Figure 5.4: RG flow diagrams of the susceptibility for the various block spin rules for $(n, m) = (n, n + 1)$. Note the odd behaviour of initial points for the temperature points above T_c, as well as the large fluctuations of T_c.

Chapter 6

Summary and conclusions

6.1 Summary

We have considered five different block spin rules for a numerical Monte Carlo Kadanoff renormalisation of a 512×512 Ising lattice. Critical exponents were calculated from the magnetisation and the magnetic susceptibility using scaling relations between the different renormalisation iterations. Critical exponents were also calculated in the same manner for lattices of varying system size that used no renormalisation.

For the magnetisation, the renormalisation methods yielded on average 4.8 values at four significant figures per method, while the finite size amount was 5. For the susceptibility, this number was 2.0 and 1.0 respectively. Thus, the renormalisation methods provided yielded no benefits for the magnetisation. Although not definitive, the renormalisation methods yielded one more result within four significant figures than for the susceptibility compared to the finite size method. We could also see that the finite size method only yielded one entry per magnetisation and susceptibility respectively within four significant figures outside the first generation, whereas the renormalisation method spread out up to the fifth generation.

The magnetisation yielded almost three times more results within the limit than the susceptibility, although 83% of these where larger than y_h compared to 55% for the susceptibility. This implied biased results for the magnetisation. It is possible this bias is due to the use of absolute magnetisation, as the results, in general, were larger.

Another difference between the magnetisation and susceptibility was the almost mirroring in the stochastic methods $P33$ and $P50$. For the magnetisation, $P33$ accounted for 34%, while $P50$ only 7%. On the other hand, for the susceptibility, $P50$ accounted for 36%, while $P33$ only 9%.

For the susceptibility, $P50$ yielded the best results, when $m-n$ is an even number. The magnetisation generally tended to prefer larger differences in iterations, with the preferred being $(n, m) = (1, 5)$. One block spin rule stood out in particular, $P33$, for iterations $(n, m) = (n, 6)$, for all n, where all values gave four correct significant figures.

6.2 Conclusions

While inconclusive, we have shown that renormalisation offered some improvement to regular finite size scaling for the susceptibility and different block spin rules worked well for different quantities. The susceptibility showed greater accuracy compared to the magnetisation although the magnetisation generated a higher quantity of close values to y_h.

In order to ascertain the usefulness of renormalisation, it may also be of interest to run simulations with initial conditions other than random states.

A natural next step would also be to implement the rules onto a 3D Ising model, especially the $P33$ rule for the magnetisation.

Appendix A

Results for $T = T_C$

A.1 y_h for the majority rule, MJ

(n, m)	$y_{h\,M}$	Percent error	Variance	$y_{h\,\chi}$	Percent error	Variance
$(1, 2)$	1.874435	0.030126	0.000004	1.877170	0.115729	0.000034
$(1, 3)$	1.874450	0.029324	0.000001	1.876610	0.085848	0.000009
$(1, 4)$	1.876151	0.061364	0.000000	1.873125	0.099984	0.000004
$(1, 5)$	1.875201	0.010726	0.000000	1.875570	0.030393	0.000002
$(1, 6)$	1.875289	0.015396	0.000000	1.876724	0.091953	0.000001
$(1, 7)$	1.876420	0.075719	0.000000	1.880388	0.287359	0.000001
$(2, 3)$	1.874465	0.028523	0.000004	1.876049	0.055968	0.000033
$(2, 4)$	1.877008	0.107109	0.000001	1.871103	0.207840	0.000008
$(2, 5)$	1.875456	0.024343	0.000000	1.875037	0.001947	0.000004
$(2, 6)$	1.875502	0.026777	0.000000	1.876613	0.086009	0.000002
$(2, 7)$	1.876817	0.096888	0.000000	1.881032	0.321686	0.000001
$(3, 4)$	1.879551	0.242740	0.000004	1.866157	0.471647	0.000032
$(3, 5)$	1.875952	0.050776	0.000001	1.874530	0.025063	0.000008
$(3, 6)$	1.875848	0.045210	0.000000	1.876800	0.096022	0.000003
$(3, 7)$	1.877405	0.128241	0.000000	1.882277	0.388115	0.000002
$(4, 5)$	1.872353	0.141188	0.000003	1.882904	0.421521	0.000030
$(4, 6)$	1.873996	0.053555	0.000001	1.882122	0.379857	0.000007
$(4, 7)$	1.876689	0.090075	0.000000	1.887651	0.674702	0.000003
$(5, 6)$	1.875639	0.034078	0.000003	1.881341	0.338193	0.000030
$(5, 7)$	1.878857	0.205706	0.000001	1.890024	0.801293	0.000007
$(6, 7)$	1.882075	0.377333	0.000002	1.898707	1.264393	0.000027

Table A.1: Results for the majority rule at $T = T_c$ using equations (3.18) for magnetisation and (3.17) for the susceptibility.

A.2 y_h for the modified majority rule, MZ

(n, m)	$y_{h\,M}$	Percent error	Variance	$y_{h\,\chi}$	Percent error	Variance
$(1, 2)$	1.877142	0.114260	0.000004	1.871003	0.213179	0.000035
$(1, 3)$	1.875926	0.049392	0.000001	1.873936	0.056735	0.000009
$(1, 4)$	1.875851	0.045361	0.000000	1.873440	0.083220	0.000004
$(1, 5)$	1.875651	0.034731	0.000000	1.875762	0.040620	0.000002
$(1, 6)$	1.876201	0.064056	0.000000	1.875015	0.000796	0.000001
$(1, 7)$	1.877119	0.113011	0.000000	1.878573	0.190567	0.000001
$(2, 3)$	1.874710	0.015476	0.000004	1.876870	0.099709	0.000033
$(2, 4)$	1.875205	0.010912	0.000001	1.874658	0.018241	0.000008
$(2, 5)$	1.875154	0.008221	0.000000	1.877348	0.125219	0.000004
$(2, 6)$	1.875966	0.051505	0.000000	1.876018	0.054289	0.000002
$(2, 7)$	1.877114	0.112761	0.000000	1.880087	0.271316	0.000001
$(3, 4)$	1.875699	0.037299	0.000003	1.872446	0.136190	0.000032
$(3, 5)$	1.875376	0.020070	0.000001	1.877587	0.137974	0.000008
$(3, 6)$	1.876384	0.073832	0.000000	1.875734	0.039149	0.000003
$(3, 7)$	1.877715	0.144821	0.000000	1.880892	0.314218	0.000002
$(4, 5)$	1.875053	0.002841	0.000003	1.882728	0.412138	0.000031
$(4, 6)$	1.876727	0.092099	0.000001	1.877378	0.126819	0.000008
$(4, 7)$	1.878387	0.180661	0.000000	1.883707	0.464354	0.000003
$(5, 6)$	1.878400	0.181357	0.000003	1.872028	0.158501	0.000030
$(5, 7)$	1.880054	0.269571	0.000001	1.884196	0.490462	0.000007
$(6, 7)$	1.881708	0.357786	0.000002	1.896364	1.139425	0.000027

Table A.2: Results for the modified majority rule at $T = T_c$ using equations (3.18) for magnetisation and (3.17) for the susceptibility. Deviation in percent from $y_h = 1.875$.

A.3 y_h for the nearest neighbour rule, NN

(n, m)	$y_{h\,M}$	Percent error	Variance	$y_{h\,\chi}$	Percent error	Variance
$(1, 2)$	1.874958	0.002234	0.000004	1.873497	0.080169	0.000033
$(1, 3)$	1.875082	0.004392	0.000001	1.874168	0.044356	0.000008
$(1, 4)$	1.875730	0.038947	0.000000	1.871994	0.160312	0.000004
$(1, 5)$	1.875655	0.034937	0.000000	1.874271	0.038902	0.000002
$(1, 6)$	1.875902	0.048107	0.000000	1.876108	0.059078	0.000001
$(1, 7)$	1.876684	0.089833	0.000000	1.879889	0.260761	0.000001
$(2, 3)$	1.875207	0.011018	0.000004	1.874840	0.008544	0.000033
$(2, 4)$	1.876116	0.059537	0.000001	1.871243	0.200384	0.000008
$(2, 5)$	1.875887	0.047328	0.000000	1.874529	0.025146	0.000004
$(2, 6)$	1.876138	0.060692	0.000000	1.876760	0.093890	0.000002
$(2, 7)$	1.877030	0.108246	0.000000	1.881168	0.328948	0.000001
$(3, 4)$	1.877026	0.108057	0.000003	1.867646	0.392224	0.000032
$(3, 5)$	1.876228	0.065482	0.000001	1.874373	0.033447	0.000008
$(3, 6)$	1.876448	0.077250	0.000000	1.877401	0.128035	0.000003
$(3, 7)$	1.877485	0.132553	0.000000	1.882750	0.413320	0.000002
$(4, 5)$	1.875430	0.022908	0.000003	1.881100	0.325330	0.000031
$(4, 6)$	1.876160	0.061846	0.000001	1.882278	0.388164	0.000007
$(4, 7)$	1.877638	0.140718	0.000000	1.887784	0.681835	0.000003
$(5, 6)$	1.876890	0.100784	0.000003	1.883456	0.450998	0.000028
$(5, 7)$	1.878743	0.199623	0.000001	1.891127	0.860088	0.000007
$(6, 7)$	1.880596	0.298462	0.000002	1.898797	1.269178	0.000027

Table A.3: Results for the nearest neighbour rule at $T = T_c$ using equations (3.18) for magnetisation and (3.17) for the susceptibility. Deviation in percent from $y_h = 1.875$.

A.4 y_h for the probabilistic 33 nearest neighbour rule, $P33$

(n, m)	$y_{h\,M}$	Percent error	Variance	$y_{h\,\chi}$	Percent error	Variance
$(1, 2)$	1.874333	0.035552	0.000004	1.876720	0.091733	0.000033
$(1, 3)$	1.875736	0.039268	0.000001	1.873334	0.088854	0.000009
$(1, 4)$	1.875035	0.001885	0.000000	1.875673	0.035911	0.000004
$(1, 5)$	1.875088	0.004675	0.000000	1.875821	0.043777	0.000002
$(1, 6)$	1.875164	0.008764	0.000000	1.878676	0.196049	0.000001
$(1, 7)$	1.876543	0.082292	0.000000	1.879966	0.264836	0.000001
$(2, 3)$	1.877139	0.114089	0.000004	1.869948	0.269441	0.000034
$(2, 4)$	1.875386	0.020603	0.000001	1.875150	0.008000	0.000008
$(2, 5)$	1.875339	0.018084	0.000000	1.875521	0.027791	0.000004
$(2, 6)$	1.875372	0.019843	0.000000	1.879165	0.222128	0.000002
$(2, 7)$	1.876985	0.105861	0.000000	1.880615	0.299456	0.000001
$(3, 4)$	1.873633	0.072882	0.000004	1.880352	0.285442	0.000033
$(3, 5)$	1.874439	0.029919	0.000001	1.878308	0.176407	0.000008
$(3, 6)$	1.874783	0.011572	0.000000	1.882237	0.385984	0.000003
$(3, 7)$	1.876946	0.103804	0.000000	1.883282	0.441681	0.000002
$(4, 5)$	1.875245	0.013045	0.000003	1.876263	0.067373	0.000032
$(4, 6)$	1.875358	0.019084	0.000001	1.883180	0.436255	0.000008
$(4, 7)$	1.878051	0.162699	0.000000	1.884258	0.493760	0.000003
$(5, 6)$	1.875471	0.025122	0.000003	1.890096	0.805138	0.000031
$(5, 7)$	1.879454	0.237526	0.000001	1.888255	0.706954	0.000007
$(6, 7)$	1.883436	0.449929	0.000002	1.886414	0.608770	0.000027

Table A.4: Results for the probabilistic 33 nearest neighbour rule at $T = T_c$ using equations (3.18) for magnetisation and (3.17) for the susceptibility. Deviation in percent from $y_h = 1.875$.

A.5 y_h for the probabilistic 50 nearest neighbour rule, $P50$

(n, m)	$y_{h\,M}$	Percent error	Variance	$y_{h\,\chi}$	Percent error	Variance
$(1, 2)$	1.873332	0.088985	0.000004	1.883889	0.474067	0.000035
$(1, 3)$	1.874517	0.025753	0.000001	1.875348	0.018582	0.000009
$(1, 4)$	1.875699	0.037283	0.000000	1.873120	0.100248	0.000004
$(1, 5)$	1.875310	0.016518	0.000000	1.875289	0.015436	0.000002
$(1, 6)$	1.875699	0.037300	0.000000	1.877009	0.107155	0.000001
$(1, 7)$	1.876619	0.086366	0.000000	1.880160	0.275208	0.000001
$(2, 3)$	1.875703	0.037478	0.000004	1.866808	0.436903	0.000035
$(2, 4)$	1.876883	0.100416	0.000001	1.867736	0.387406	0.000008
$(2, 5)$	1.875969	0.051685	0.000000	1.872423	0.137441	0.000004
$(2, 6)$	1.876291	0.068871	0.000000	1.875289	0.015427	0.000002
$(2, 7)$	1.877277	0.121436	0.000000	1.879414	0.235437	0.000001
$(3, 4)$	1.878063	0.163355	0.000003	1.868664	0.337909	0.000032
$(3, 5)$	1.876102	0.058789	0.000001	1.875230	0.012289	0.000008
$(3, 6)$	1.876488	0.079336	0.000000	1.878116	0.166204	0.000003
$(3, 7)$	1.877670	0.142426	0.000000	1.882566	0.403522	0.000002
$(4, 5)$	1.874142	0.045777	0.000003	1.881797	0.362487	0.000029
$(4, 6)$	1.875700	0.037326	0.000001	1.882842	0.418260	0.000007
$(4, 7)$	1.877540	0.135449	0.000000	1.887200	0.650665	0.000003
$(5, 6)$	1.877258	0.120429	0.000002	1.883888	0.474032	0.000028
$(5, 7)$	1.879239	0.226062	0.000001	1.889902	0.794754	0.000007
$(6, 7)$	1.881219	0.331696	0.000002	1.895915	1.115476	0.000026

Table A.5: Results for the probabilistic 50 nearest neighbour rule at $T = T_c$ using equations (3.18) for magnetisation and (3.17) for the susceptibility. Deviation in percent from $y_h = 1.875$.

A.6 y_h for finite size scaling, FZ

(n, m)	$y_{h\,M}$	Percent error	Variance	$y_{h\,\chi}$	Percent error	Variance
$(1, 2)$	1.873630	0.073046	0.000004	1.877001	0.106730	0.000035
$(1, 3)$	1.874977	0.001221	0.000001	1.871857	0.167651	0.000009
$(1, 4)$	1.875171	0.009119	0.000000	1.873918	0.057705	0.000004
$(1, 5)$	1.875327	0.017431	0.000000	1.874863	0.007311	0.000002
$(1, 6)$	1.875361	0.019241	0.000000	1.877246	0.119789	0.000001
$(1, 7)$	1.876988	0.106026	0.000000	1.878582	0.191040	0.000001
$(2, 3)$	1.876324	0.070604	0.000004	1.866712	0.442033	0.000033
$(2, 4)$	1.875941	0.050202	0.000001	1.872376	0.139923	0.000008
$(2, 5)$	1.875892	0.047590	0.000000	1.874150	0.045325	0.000004
$(2, 6)$	1.875793	0.042313	0.000000	1.877307	0.123054	0.000002
$(2, 7)$	1.877660	0.141841	0.000000	1.878898	0.207902	0.000001
$(3, 4)$	1.875559	0.029799	0.000003	1.878041	0.162187	0.000032
$(3, 5)$	1.875677	0.036082	0.000001	1.877869	0.153029	0.000008
$(3, 6)$	1.875617	0.032883	0.000000	1.880839	0.311416	0.000003
$(3, 7)$	1.877993	0.159650	0.000000	1.881945	0.370386	0.000002
$(4, 5)$	1.875794	0.042366	0.000003	1.877698	0.143872	0.000032
$(4, 6)$	1.875645	0.034424	0.000001	1.882238	0.386030	0.000008
$(4, 7)$	1.878805	0.202933	0.000000	1.883246	0.439786	0.000003
$(5, 6)$	1.875497	0.026483	0.000003	1.886779	0.628188	0.000029
$(5, 7)$	1.880310	0.283217	0.000001	1.886020	0.587743	0.000007
$(6, 7)$	1.885124	0.539952	0.000002	1.885262	0.547298	0.000026

Table A.6: Results for the finite size scaling at $T = T_c$ using equations (3.18) for magnetisation and (3.17) for the susceptibility. Deviation in percent from $y_h = 1.875$.

Bibliography

[1] W. Lenz, "Beiträge zum verständnis der magnetischen eigenschaften in festen körpern," *Physikalische Zeitschrift*, vol. 21, pp. 613–615, 1920.

[2] E. Ising, "Beitrag zur theorie des ferromagnetismus," *Zeitschrift für Physik*, vol. 31, no. 1, pp. 253–258, 1925.

[3] L. Onsager, "Crystal statistics. i. a two-dimensional model with an order-disorder transition," *Physical Review*, vol. 65, no. 3-4, pp. 117–149, 1944.

[4] R. Peierls, "On ising's model of ferromagnetism," *Mathematical Proceedings of the Cambridge Philosophical Society*, vol. 32, no. 3, pp. 477–481, 1936.

[5] M. E. Fisher, "The theory of equilibrium critical phenomena," *Reports on Progress in Physics*, vol. 30, no. 2, pp. 615–730, 1967.

[6] S. Blundell, *Concepts in thermal physics*. Oxford: Oxford University Press, 2nd ed.. ed., 2010.

[7] W. Wagner and A. Pruss, "The iapws formulation 1995 for the thermodynamic properties of ordinary water substance for general and scientific use," *Journal of Physical and Chemical Reference Data*, vol. 44, no. 1, p. 1, 2015.

[8] R. B. Griffiths, "Dependence of critical indices on a parameter," *Physical Review Letters*, vol. 24, no. 26, pp. 1479–1482, 1970.

[9] K. G. Wilson, "The renormalization group and critical phenomena," *Reviews of Modern Physics*, vol. 55, no. 3, pp. 583–600, 1983.

[10] L. P. Kadanoff, "Scaling laws for ising models near T_c," *Physics Physique Fizika*, vol. 2, pp. 263–272, Jun 1966.

[11] M. Plischke, *Equilibrium statistical physics*. Singapore: World Scientific, 3. ed.. ed., 2006.

[12] D. Ron, A. Brandt, and R. H. Swendsen, "Surprising convergence of the monte carlo renormalization group for the three-dimensional ising model.," *Physical review. E*, vol. 95, no. 5-1, pp. 053305–053305, 2017.

[13] M. Kikuchi and Y. Okabe, "A Simple Method of Monte Carlo Renormalization Group," *Progress of Theoretical Physics*, vol. 75, pp. 192–194, 01 1986.

[14] M. Kikuchi and Y. Okabe, "A Scaling Approach to Monte Carlo Renormalization Group," *Progress of Theoretical Physics*, vol. 78, pp. 540–551, 09 1987.

[15] L. E. Ballentine, *Quantum mechanics : a modern development*. 2nd edition.. ed., 2015.

[16] T. Schultz, D. Mattis, and E. Lieb, "Two-dimensional ising model as a soluble problem of many fermions," *Reviews of Modern Physics*, vol. 36, no. 3, pp. 856–871, 1964.

[17] M. Campostrini, A. Pelissetto, P. Rossi, and E. Vicari, "25th-order high-temperature expansion results for three-dimensional ising-like systems on the simple-cubic lattice," *Physical Review E*, vol. 65, Jun 2002.

[18] G. S. Rushbrooke, "On the thermodynamics of the critical region for the ising problem," *The Journal of Chemical Physics*, vol. 39, no. 3, pp. 842–843, 1963.

[19] B. Widom, "Degree of the critical isotherm," *The Journal of Chemical Physics*, vol. 41, no. 6, pp. 1633–1634, 1964.

[20] R. B. Griffiths, "Thermodynamic inequality near the critical point for ferromagnets and fluids," *Physical Review Letters*, vol. 14, no. 16, pp. 623–624, 1965.

[21] M. E. Fisher, "Rigorous inequalities for critical-point correlation exponents," *Physical Review*, vol. 180, no. 2, pp. 594–600, 1969.

[22] R. H. Swendsen, "Monte carlo renormalization group," *Physical Review Letters*, vol. 42, no. 14, pp. 859–861, 1979.

[23] R. H. Swendsen, "Monte carlo calculation of renormalized coupling parameters," *Phys. Rev. Lett.*, vol. 52, pp. 1165–1168, Apr 1984.

[24] C. Baillie, R. Gupta, K. Hawick, and G. Pawley, "Monte-carlo renormalization-group study of the 3-dimensional ising-model," *Physical Review B*, vol. 45, no. 18, pp. 10438–10453, 1992.

[25] Y. Wu and R. Car, "Variational approach to monte carlo renormalization group.," *Physical review letters*, vol. 119, no. 22, pp. 220602–220602, 2017.

[26] N. Metropolis, A. W. Rosenbluth, M. N. Rosenbluth, A. H. Teller, and E. Teller, "Equation of state calculations by fast computing machines," *The Journal of Chemical Physics*, vol. 21, no. 6, pp. 1087–1092, 1953.

[27] Swendsen and Wang, "Nonuniversal critical dynamics in monte carlo simulations," *Physical review letters*, vol. 58, no. 2, p. 86, 1987.

[28] Wolff, "Collective monte carlo updating for spin systems," *Physical review letters*, vol. 62, no. 4, p. 361, 1989.

[29] B. A. Berg, "Introduction to markov chain monte carlo simulations and their statistical analysis." arXiv:cond-mat/0410490v1, 2004.

TRITA SCI-GRU 2020:043